



Available Online at EScience Press

International Journal of Phytopathology

ISSN: 2312-9344 (Online), 2313-1241 (Print)
<https://esciencepress.net/journals/phytopath>

DETECTION AND MOLECULAR CHARACTERIZATION OF PHYTOPLASMA ASSOCIATED WITH PHYLLODY DISEASE ON *DIMORPHOTHECA PLUVIALIS* IN EGYPT

^aOm-Hashem M. El-Banna, ^bAhmed A. Kheder, ^{c,d}Mayadah A. Haj Ali

^a Department of Plant Pathology, Faculty of Agriculture, Cairo University, Egypt.

^b Department of Virus and Phytoplasma, Plant Pathology Research Institute, Agricultural Research Centre (ARC), Egypt.

^c International Centre for Agricultural Research in the Dry Areas (ICARDA), Giza, Egypt.

^d Department of Microbiology and Immunology, National Commission for Biotechnology (NCBT), Damascus, Syria.

ARTICLE INFO

Article History

Received: November 11, 2023

Revised: March 27, 2024

Accepted: April 22, 2024

Keywords

Dimorphotheca pluvialis

Phytoplasma

Phyllody disease

PCR

TEM

Ultrastructural changes

ABSTRACT

During the spring of 2021-2022, imported grown African daisy (*Dimorphotheca pluvialis* L. Moench) plants (Family: Asteraceae) exhibiting symptoms of phyllody phytoplasma, such as phyllody and virescence of flowers, and witches' broom, were observed in different gardens of Cairo governorate, Egypt. The disease was successfully transmitted experimentally through dodder (*Cuscuta reflexa*) to healthy periwinkle (*Cantharanthus roseus*) plants. The light and transmission electron microscopic examination revealed phytoplasma units in sieve tubes with a lot of deterioration of the cell components due to the phytoplasma infection. Nested polymerase chain reaction (nested-PCR) assay used as a key technique to identify the phytoplasma by amplifying products of 1250 bp using two pairs of primers; a universal primer pair (P1/P7) and (R16F2n/R16R2) as a specific primer pair. The Egyptian phytoplasma isolate (Dimo-Cairo) was registered with accession number "OQ676407.1" in the NCBI GenBank. MEGA sequence analysis software version 11 was used to generate the phylogenetic tree of Dimo-Cairo and to compare it with the other phytoplasma strains. The clustering of phytoplasma strains confirmed that Dimo-Cairo was associated with the 16Sr-II group (*Candidatus* Phytoplasma *aurantifolia*), and placed it close to stem curling and phyllody phytoplasma (16Sr-II-A subgroup), witches-broom phytoplasma and cactus witches-broom phytoplasma (16Sr-II-C subgroup) and *Corchorus olitorius* phytoplasma and *Vicia faba* stunting phytoplasma (16Sr-II-D subgroup). To our knowledge, this is the first report of a phytoplasma infecting *Dimorphotheca pluvialis* plants in Egypt.

Corresponding Author: Mayadah A. Haj Ali

Email: mayyada.hajali@gmail.com

© The Author(s) 2024.

INTRODUCTION

Phytoplasma is a wall-less phytopathogenic mollicute colonizing the plant phloem and insects (Lee *et al.*, 2000), thus it is transmitted experimentally by vegetative propagation; grafting, insect vectors; especially leafhoppers and plant parasitic species (dodder) (Salehi *et al.*, 2005; El-Banna *et al.*, 2015; Gad *et al.*, 2019). Naturally, phytoplasma is one of the serious

devastating microorganisms in several ornamental plants. There are many phytoplasma species such as 16Sr-IB and 16Sr-IC phytoplasma subgroups showing virescence and yellow stunted leaves in cyclamen (*Cyclamen persicum* L.) (Alma *et al.*, 2000), *Candidatus* phytoplasma *asteris* in cyclamen (Viczián *et al.*, 2023), 16Sr-I-R phytoplasma associated with phyllody disease in *Aquilegia vulgaris* (Family

Ranunculaceae) (Babaei *et al.*, 2021), 16SrI-B, 16SrII-C, 16Sr II-D and 16SrXIV-A phytoplasma subgroups associated with witches' broom and leaf yellowing disease infecting different eleven bamboo species (Ravi *et al.*, 2022), 16SrIII-J phytoplasma showing dwarfing, witches' broom and chlorosis symptoms in cassava (*Manihot esculenta* Crantz) (Fernández *et al.*, 2018), *Candidatus* phytoplasma *asteris* (*Ca. P. astris*) associated with severe fasciation symptoms in lily (*Lilium* spp.) plants (Bertaccini *et al.*, 2005), *Candidatus* phytoplasma *asteris* association with leaf yellowing of *Wrightia antidysenterica* (also known as 'Arctic Snow') (Family Poinciaceae) (Shreenath *et al.*, 2021), *Candidatus* phytoplasma *malaysianum* (16SrXXXII) associated with a decline disease affecting the leaves and seeds of *E. sylvestris* (Family *Elaeocarpaceae*) (Lee *et al.*, 2022), aster yellows phytoplasma associated with a little leaf disease in papaya (*Carica papaya* L.) plant (Mitra *et al.*, 2020), *Candidatus* Phytoplasma *australasia* associated with little leaf and yellowing symptoms in *Pyracantha angustifolia* (Family: *Rosaceae*) (Kilic *et al.*, 2022), *Candidatus* phytoplasma *fraxini*' associated with witches' broom disease in *Erigeron bonariensis* (Montano *et al.*, 2014), *Chrysanthemum* yellows phytoplasma infecting *Arabidopsis thaliana* wild type and *Atcal57ko* mutant plants (Bernardini *et al.*, 2022), *Coreopsis grandiflora* phyllody phytoplasma infecting pot marigold (*Calendula officinalis* L., family *Asteraceae*) and tickseed (*Coreopsis grandiflora*) (Gharouni-Kardani *et al.*, 2020), *Candidatus* Phytoplasma *asteris* associated with yellows disease in gerbera (*Gerbera jamesonii*) (commonly known as African daisy) (family *Asteraceae*) (Gautam *et al.*, 2020), *Candidatus* Phytoplasma *asteris*' strain associated with phyllody disease in pot marigold (Family *Asteraceae*) (Salehi *et al.*, 2022; Gharouni-Kardani *et al.*, 2020; Esmailzadeh Hosseini *et al.*, 2018) and jujube witches'-broom (JWB) phytoplasma in periwinkle (*Cantharanthus roseus*) plant (Lee *et al.*, 2012). In Egypt, phytoplasma infecting lilies (*Lilium* spp.) (Abdel-Salam *et al.*, 2022), *Dodonaea viscosa* (Mokbel, 2020), gazania (Gad *et al.*, 2019), *Cycas revoluta* (Behiry, 2018) and rose plants (Mikhail *et al.*, 2012). All the above phytoplasma infections cause significant losses in the yield quantity and quality of infected plants.

In the spring of 2021-2022, unusual symptoms were observed on African daisy plants (*Dimorphotheca pluvialis* L. Moench) grown in different gardens in Cairo governorate, Egypt. These symptoms included phyllody

and virescence of flowers, and witches' broom similar to phytoplasma infection.

Due to the difficulty of the phytoplasma culturing on artificial media, the detection methods are still restricted. So, light microscopy and transmission electron microscopy (TEM) are used to check the presence of phytoplasma in the vascular bundles of the phloem tissues in the ultrathin sections as stated by El-Banna *et al.* (2015).

Recently, molecular techniques which overcome problem of low concentration of phytoplasma in the infected phloem tissues by increasing sensitivity and specificity of detection as mentioned by Gundersen and Lee (1996). These techniques, such as Nested-Polymerase Chain Reaction (Nested-PCR) and sequence analysis, proved successful in identifying phytoplasma strains through amplifying the 16S ribosomal RNA (16S rRNA) gene as described by Deng and Hiruki (1991) and Sinclair *et al.* (1996).

The objective of this research is the identification and prove responsibility of phytoplasma of the disease symptoms observed on the candidate plants, which represents a threat in African daisy plants for the first time in Egypt, using biological and molecular characterizations.

MATERIALS AND METHODS

Sampling

Five symptomatic African daisy plants were collected from some gardens of Cairo governorate during the growing season 2021-2022. These symptoms included phyllody, virescence, and witches' broom. The suspected plants were collected and replanted in plastic pots (20 cm) and kept in the greenhouse of the Department of Virus and Phytoplasma, Plant Pathology Research Institute, Agricultural Research Centre (ARC), Giza, Egypt until further use.

Detection and Characterization of Phytoplasma Pathogenicity Test

Dodder (*Cuscuta reflexa*) seeds were germinated on wet filter paper in the petri dishes (12 cm in diameter) for 1 week at room temperature (22-25 °C) according to El-Banna *et al.* (2007).

Then, the germinated dodder seeds were placed on the stems of naturally infected African daisy plants (5 germinated seeds/ plant) grown in ten plastic pots (20 cm) containing a mixture of vermiculite and peatmoss (1:1) (Gad *et al.*, 2019). Dodder plants were allowed to

parasitize 10 healthy periwinkle plants. Plants were grown under cages in greenhouse and observed for symptoms appearance. Percentage of dodder transmission was calculated as:

Number of symptomatic periwinkle plants /number of tested periwinkle x100.

The presence of phytoplasma in the symptomatic new leaves was confirmed depending on phytoplasma phenotypical symptoms.

Histopathological Changes

The protocols described by El-Banna *et al.* (2020), Hunter *et al.* (1993) and El-Banna and El-Deeb (2007) were followed for the anatomical and ultrastructural changes induced in the petioles midribs of the naturally infected African daisy plant using light microscopy and transmission electron microscopy (TEM), respectively at the transmission electron microscope (TEM) lab, Research Park (FARP), Faculty of Agriculture, Cairo University, Egypt.

Preparing of the Plant Tissue for Examination

Pieces of about 2 x 2 mm of the infected leaf midribs were fixed in 2.5% glutaraldehyde in 0.1 M sodium phosphate buffer (pH 7.4) for one hour. After removing the fixative solution, the tissues were washed in sodium phosphate buffer three times for 30 min each. Then refixed in 1% of Osmium-tetroxide (OsO₄) for 1.5 h at 4°C. Then the samples were dehydrated in an ethanol series of 15%, 30%, 50%, 70%, 80% and 95%, before exposing to 100% for 15 minutes for every step except the step of 100% ethanol, which was repeated twice. Infiltration with Spur's epoxy resin, one large drop into the sample tube every 15 minutes, until at 75% resin overnight with rotating. Samples were put into 100% resin, for at least a day, and then samples

were placed into flat BEEM capsule molds, hardening the resin was done overnight in an oven at 60°C according to the steps explained by El-Banna *et al.* (2020).

Light Microscopy

The prepared samples were then sectioned (500-1000 µm thick) with an ultra-microtome (Leica model EM-UC6, Japan). Sections were stained with a few drops of 1% alkaline toluidine blue and were examined by light microscope (Leica ICC50 HD) at the candidate magnification to 10x as described previously by Hunter *et al.* (1993).

Electron Microscopy of Ultra-Thin Sections

The prepared samples were then sectioned (90-100 nm thick) with an ultra-microtome (Leica model EM-UC6, Japan) mounted on copper grids (400 mesh). Sections were double stained with 2% Uranyl acetate and 10% lead citrate according the method described by El-Banna and El-Deeb (2007) and 2020) El-Banna *et al.* (2020). Stained sections were detected using transmission Electron microscope JEOL (JEM-1400 TE, Japan) at the candidate magnification. Images were captured using CCD camera model AMT.

Molecular Characterization of Phytoplasma

DNA Extraction

Total DNA was extracted from healthy and infected African daisy plants using the modified Dellaporta extraction method (Dehestani and Tabar, 2007).

Nested - Polymerase Chain Reaction (Nested-PCR)

Universal phytoplasma primers (P1/ P7) and specific primers (R16F2n/ R16R2) were used to amplify 1.8 and 1.2 kb for first PCR and second PCR, respectively of the 16S ribosomal RNA as described previously by Sinclair *et al.* (1996). The sequence of the used primer pairs is illustrated in Table 1.

Table 1. Primers sequences, specificity used for nested PCR and expected amplification size.

Primer	Specificity	Primer sequence (5' to 3')	Expected amplification size (bp)
P1	Universal	5'-AAGAGTTTGATCCTGGCTCAGGATT-3'	1800
P7		5'-CGTCCTTCATCGGCTCTT-3'	
R16F2	Nested	5'-GAAACGACTGCTAAGACTGG-3'	1200
R16R2		5'-TGACGGGCGGTGTGTACAAACCCC-3'	

A PCR reaction was performed on a 25 µL solution containing 1 µL DNA, 12.5 µL Mangotaq DNA polymerase (Bioline GmbH, Luckenwalde), 25 pmol of each primer, and 8.5 µL of nuclease free water (Promega, USA).

The total DNA was first heat-denatured at 94°C/ 3 min, followed by 35 cycles; each were performed

(denaturation at 94°C/ 30 s, annealing at 53°C/ 1 min, and primer extension at 72°C/ 2 min) and ending with a final cycle at final extension at 72°C/ 7 min using the Labnet (MULTIGENE MINI) thermal cycler according to Deng and Hiruki (1991).

The nested PCR products were stained with EZ View

nucleic acid stain (Biomatik, Canada), electrophoresed in 1% agarose gel and visualized using a gel documentation system (TR201 UV Trans illuminator, acculab, USA).

PCR Purification, Sequencing and Phylogenetic Studies

The PCR bands of the 16S ribosomal RNA (16S rRNA) gene of the Egyptian isolate (Dimo-Cairo) was cut from the agarose gel and purified by the QIAquick® PCR Purification kit (QIAGEN, Germany).

Then they were sequenced by Sigma Company (Cairo, Egypt). The nucleotide sequence of Dimo-Cairo isolate was submitted in the GenBank to obtain accession number (OQ676407.1). The obtained sequences were assembled and compared with other reference sequences available in the GenBank using a NCBI/ BLAST.

Phylogenetic tree was performed using MEGA sequence analysis software version 11 (Tamura *et al.*, 2021).

The percentage of nucleotide identities of the 16S ribosomal RNA (16S rRNA) gene of Dimo-Cairo isolate was calculated using Sequence Demarcation tool (SDT v1.3) (Muhire *et al.*, 2014).

RESULTS

Disease Symptoms

Phytoplasma symptoms were observed on phyllody disease-infected African daisy plants grown in different gardens in Cairo governorate, Egypt. Infected plants exhibited typical symptoms of phytoplasma, such as phyllody and virescence of flowers (Figure 1A) and witches' broom (Figure 1B).



Figure 1. Naturally infected African daisy plants showing typical symptoms of phytoplasma infection: (A) phyllody and virescence of African daisy flowers and (B) African daisy witches' broom. (C) A healthy African daisy plant used as negative control.

Detection and Characterization of Phytoplasma Pathogenicity Test

Phytoplasma was successfully transmitted from infected African daisy plants to 9 healthy periwinkle plants out of total 10 tested periwinkle plants using dodder transmission, producing yellowing, virescence and phyllody after 28 days with 90% transmission rate (Figure 2B).

Dimorphotheca pluvialis phyllody phytoplasma causes yellowing disease on periwinkle plants, which is very similar to phyllody disease-infected African daisy showing chlorosis and yellowing on leaves. Infected flowers showed symptoms of phyllody and virescence on the periwinkle petals.

Histopathology

Light and transmission electron microscopy (TEM) of infected petioles midribs of African daisy plants revealed that the most histological changes occurred in the

phloem tissues.

The infected phloem tissues contained numerous vascular bundles (VB) (Figure 3A and 3B) with clear thick cell walls of the phloem cells and many necrotic areas (N) were also recognised between these cells (Figure 3C, 3D, 3F and 3G). On the other hand, some vascular bundles of infected phloem contained a lot of xylem (X) cells (Figure 3E), in addition to necrotic areas (N) between the phloem (P) cells (Figure 3E).

When revealing the phloem sites of the phytoplasma-infected African daisy plants using transmission electron microscope (TEM), many sieve elements containing numerous phytoplasma units (P) were recognized. These units were mostly rounded, elongated or pleomorphic bodies bounded by a unit membrane (Figure 4A and 4B), which was noticed in groups next to the thick cell wall and ready to pass the sieve pores (Figure 4A).



Figure 2. Dodder transmission: (A) germination of dodder seeds, (B) dodder stolon's attached from African daisy to periwinkle plants.

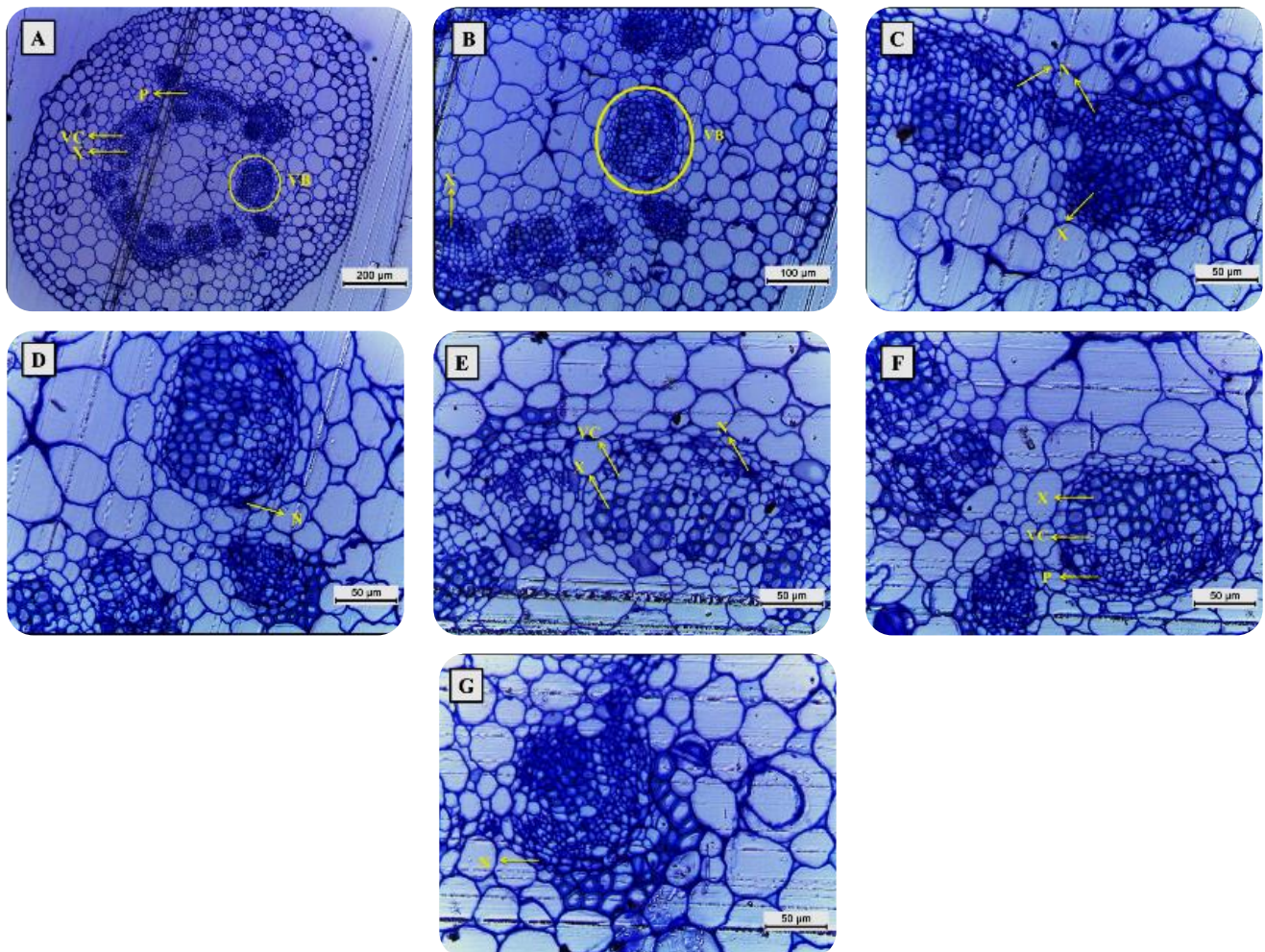


Figure 3. Cross sections of petioles midribs of the African daisy plants infected with phytoplasma. (A) Overview of infected phloem tissues with numerous vascular bundles (VB), each contained phloem (P), vascular cambium (VC) and xylem (X), at the magnifications (100x). (B) Some vascular bundles at magnification (200x). (C), (D), (F) and (G) Necrotic areas (N) were observed between the phloem cells (400x). (E) A lot of xylem cells in the infected vascular bundles (400x).

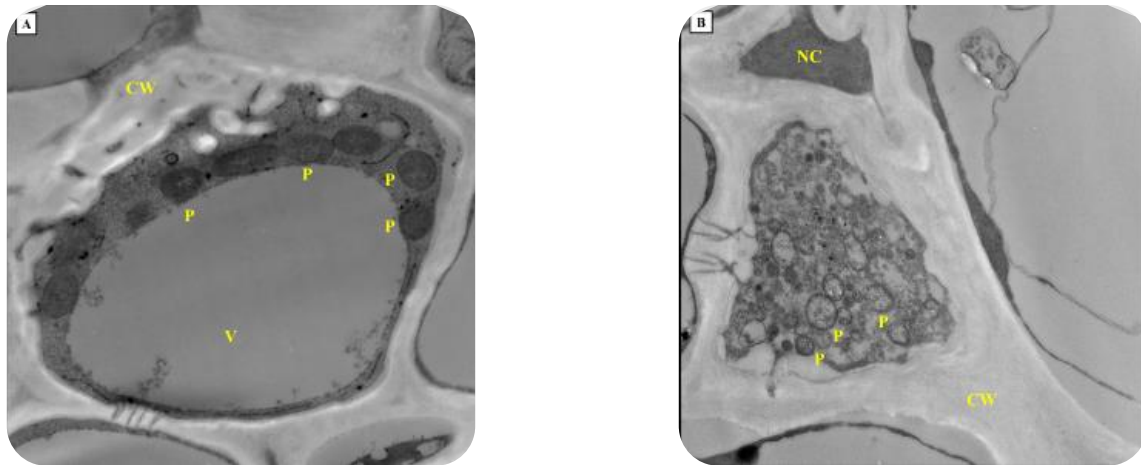


Figure 4. Transmission electron micrograph of sieve elements in the phytoplasma-infected African daisy plants. (A) Some of phytoplasma units (P) arranged next to the cell wall (CW) (12000 \times). (B) Numerous pleomorphic bodies of phytoplasma units (P) in cytoplasm of sieve element which was characterized with thick cell wall at high magnification (15000 \times).

Disorganization with abnormalities in the phloem cells (Figure 5A) was remarkable in the infected plant tissues, such as uneven thickness (Figure 5B) and an irregular shape in the cell wall with many extensions were grown. Plasmodesmata (PL) are very obvious in Figure 5C. Chloroplast of infected sieve elements was damaged

(Figure 6A), whereby their membranes were partially destroyed (Figure 6C) and grana were irregularly arranged (Figure 6B).

On the other hand, the nucleus (N) was degraded in some infected sieve elements (Figure 7B), but it kept its shape in the other infected ones (Figure 7A and 7C).

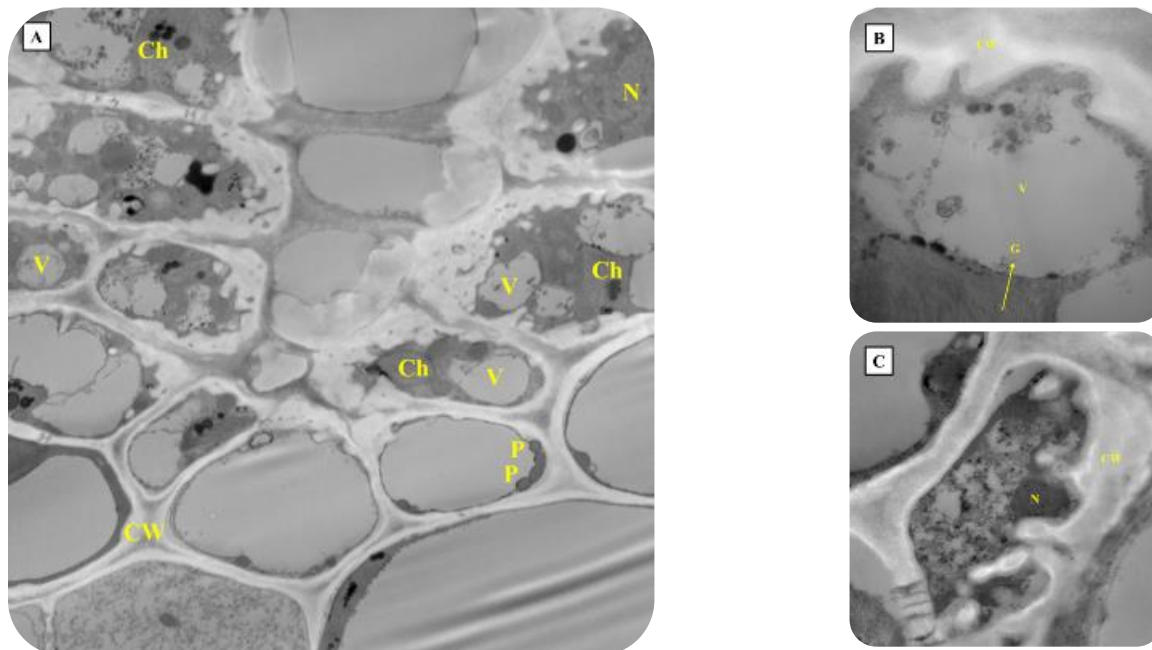


Figure 5. Transmission electron micrograph of irregular cell wall (CW) of the infected petioles midribs. (A) Overview of phytoplasma-infected phloem tissues as disorganization and abnormalities are remarkable (4000 \times). (B) The cytoplasm of the phytoplasma-infected plants was decomposed, necrotized and vacuolated (V). Uneven thickness of infected cell wall (CW) (30000 \times). (C) Irregular shape of cell wall (CW) with many growing extensions. Plasmodesmata (PL) are very obvious (20000 \times).

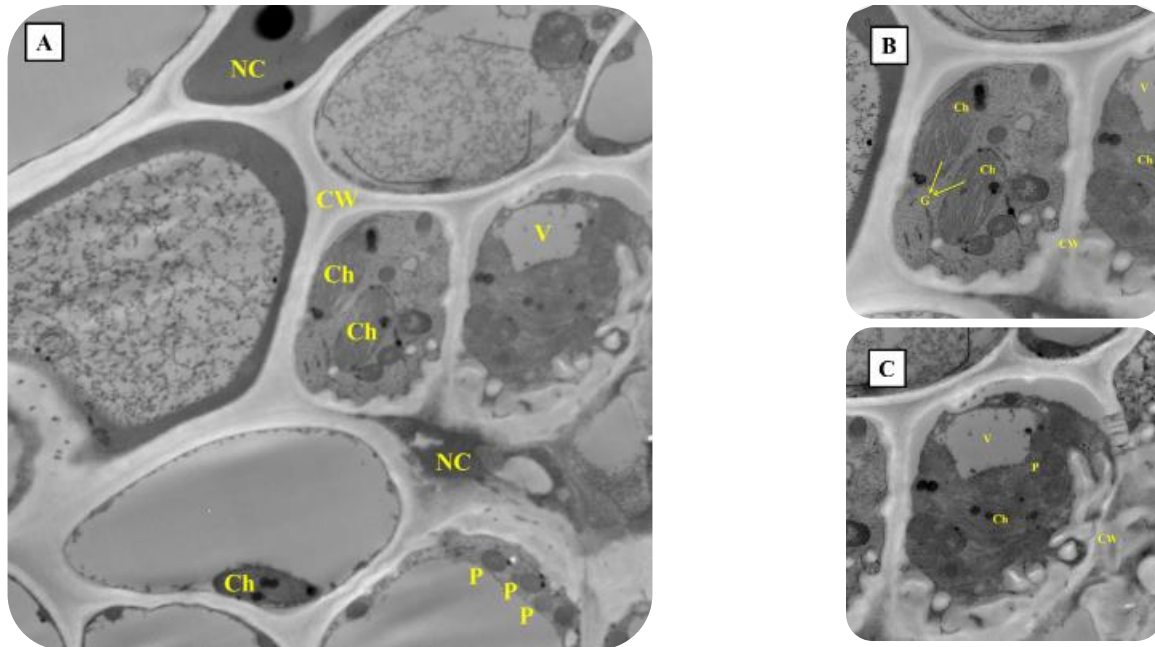


Figure 6. Transmission electron micrograph of chloroplasts degradation in the infected sieve elements. (A) Overview of chloroplasts (Ch) distribution in the infected phloem cells (5000x). (B) Irregular grana arranging (12000x). (C) Partial lysis of the damaged chloroplast's membranes (12000x).

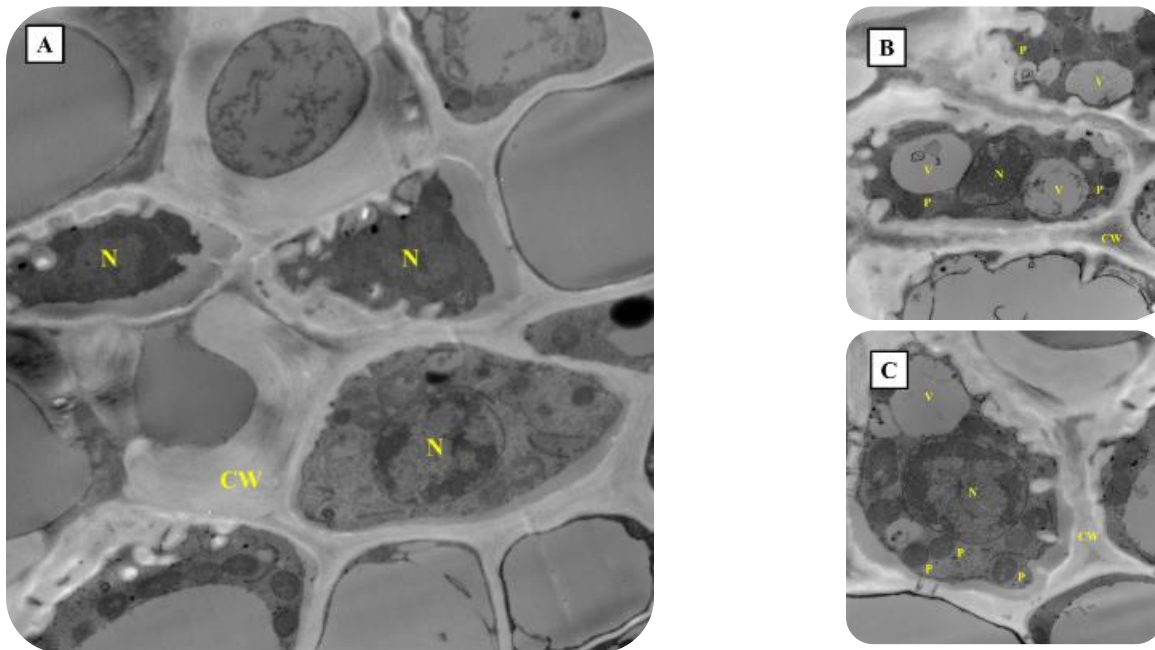


Figure 7. Transmission electron micrograph of the phytoplasma-infected petioles midribs. (A) Overview of nucleus (N) distribution in the infected phloem cells (6000x). (B) Degradation of nucleus (N) in the phytoplasma-infected phloem cell (12000x). (C) Some phytoplasma (P) in the infected sieve element was surrounded by wall appositions (12000x).

Molecular Characterization of Phytoplasma

Nested-PCR

Three samples were reacted positively with Nested-PCR out of five collected African daisy samples by forming 1250 bp bands on 1% agarose gel (Figure 8), indicating

the presence of phyllody disease in some gardens in Cairo governorate, Egypt.

Phylogenetic Study of Dimo-Cairo Isolate

The Egyptian isolate (Dimo-Cairo) was purified,

sequenced and submitted to the GenBank with accession number "OQ676407".

Phylogenetic analysis was conducted to compare Egyptian isolate (Dimo-Cairo) with the other 16S rRNA groups available in GenBank (Figure 9, Table 2), the comparison proved that Dimo-Cairo formed same

cluster with those strains of phytoplasma affiliated with subgroups in 16Sr-II group. This sequence shared 98.5 and 99.2% homology with *Candidatus Phytoplasma aurantifolia* affiliated with subgroups in 16Sr-II group from India (Access no. MT555412.1) and Iraq (Access no. KU724309.2), respectively.

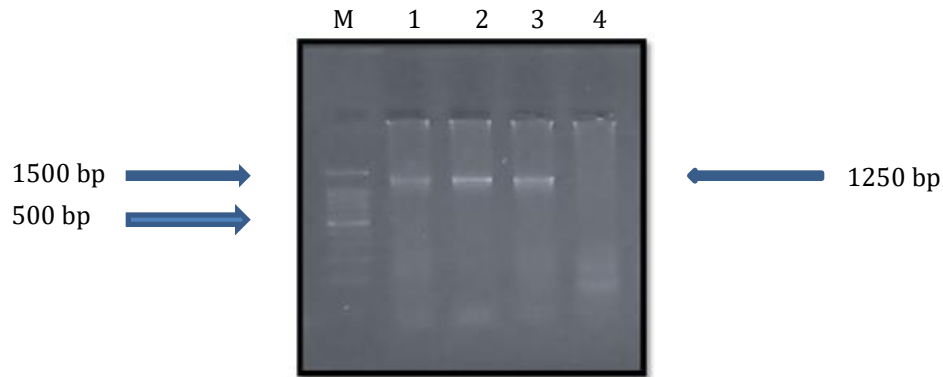


Figure 8. Agarose gel electrophoresis of nested-PCR amplification of 16S ribosomal RNA gene using 16S rRNA primer pair P1/P7 followed by R16F2n/R16R2 for *Dimorphotheca pluvialis* phyllody phytoplasma. [Lanes; M: DNA ladder (1000 bp) (Biomatic-USA), 1: *Dimorphotheca pluvialis* phyllody and virescence phytoplasma sample, 2: *Dimorphotheca pluvialis* phyllody phytoplasma sample (Dimo-Cairo), 3: *Dimorphotheca pluvialis* witches' broom phytoplasma sample, 4: Healthy *Dimorphotheca pluvialis* plant (Negative control)].

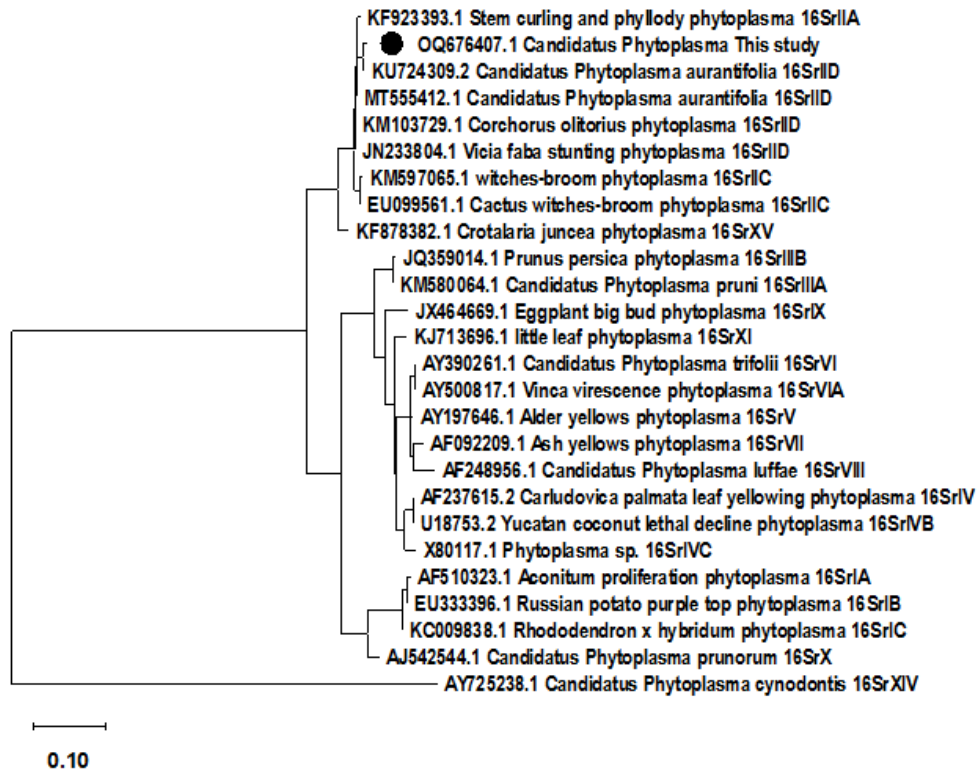


Figure 9. A phylogenetic tree of the 16S ribosomal RNA (16S rRNA) gene of Dimo-Cairo was performed using MEGA sequence analysis software version 11.

Table 2. Comparison of the Dimo-Cairo sequence with other phytoplasma reference sequences available in the GenBank.

GenBank	16Sr	Country	host	Strain	Id%
AF510323	IA	Lithuania	<i>Aconitum napellus</i> L., aconite	AcP	84.6%
EU333396	IB	Russian	<i>Solanum tuberosum</i> , potato	Rus103-1	85.0%
KC009838	IC	Czech Republic	<i>Rhododendron hybridum</i> cv.,	AzLL	85.8%
OQ676407	II	Egypt	<i>Dimorphotheca pluvialis</i>	Dimo-Cairo	
KU724309	IID	Iraq	Tomato	1	99.2%
MT555412	IID	India	<i>Croton bonplandianus</i>	CB04	98.5%
KF923393	IIA	Taiwan	<i>Sesamum indicum</i> , Sesame	ASC	98.1%
KM597065	IIC	Brazil	<i>Eucalyptus urophylla</i> , Eucalyptus	EucWB- Braz	97.7%
EU099561	IIC	China	<i>Opuntia</i> sp., cactus	YN16	97.7%
KM103729	IID	Turkey	<i>Corchorus olitorius</i> L. , Jute	JuPhy2	98.5%
JN233804	IID	Sudan	<i>Vicia faba</i> L., Faba bean	SUD-Fb4	98.5%
KM580064	IIIA	Canada	<i>Syringa x josiflexa</i> 'Charisma', Lilac	LilacS1- Canada	85.8%
JQ359014	IIIB	Argentina	<i>Prunus persica</i> L. , peach	ArPY	85.4%
AF237615	IV	Mexico	<i>Carludovica palmata</i> , palm	CPY	83.8%
U18753	IVB	Mexico	<i>Cocos nucifera</i> , coconut palms	LDY	83.8%
X80117	IVC	Tanzania	<i>Cocos nucifera</i> , coconut palms	LDT	83.1%
AY197646	V	Italy	<i>Alnus glutinosa</i> , alder	ALY	82.7%
AY390261	VI	Canada	<i>Trifolium hybridum</i> , clover	CP	82.7%
AY500817	VIA	USA	<i>Vinca minor</i> L., common periwinkle	VR	82.7%
AF092209	VII	USA	<i>Fraxinus Americana</i> , ash	AshY1	83.5%
AF248956	VIII	Taiwan	<i>Luffa</i> sp., loofah	LfWB	84.6%
JX464669	IX	Iran	<i>Solanum melongena</i> , eggplant	EPH- Iran	83.5%
AJ542544	X	Germany	<i>Prunus persica</i> , peach	ESFY-G1	86.2%
KJ713696	XI	India	<i>Jasminum sambac</i> , jasmine	Jas LY and WB	83.8%
AY725238	XIV	Cuba	<i>Cynodon dactylon</i> , Bermuda grass	BGWL-Cuba	39.6%
KF878382	XV	Brazil	<i>Crotalaria juncea</i> , sunn hemp	SHY-III	94.6%

However, the 16S rRNA gene sequence of Dimo-Cairo revealed (98.1%) identity with stem curling and phyllody phytoplasma (KF923393.1) (Taiwan); member of 16Sr-II-A subgroup, (97.7%) identity with witches-broom phytoplasma (Access no. KM597065.1) (Brazil) and cactus witches-broom phytoplasma (EU099561.1) (China); members of 16Sr-II-C subgroup, and (98.5 %) identity with *Corchorus olitorius* phytoplasma (Access no. KM103729.1) (Turkey) and *Vicia faba* stunting phytoplasma (Access no. JN233804.1) (Sudan); members of 16Sr-II-D subgroup.

Also, the percentage of nucleotide identities of Dimo-Cairo isolate was calculated using Sequence Demarcation tool (SDT v1.3) (Figure 10).

DISCUSSION

Phytoplasma is considered as a devastating phytopathogenic mollicute in several ornamental plants grown in fields, gardens and greenhouses,

causing economic yield losses, especially in the flower productions worldwide (Kilic *et al.*, 2022; Viczián *et al.*, 2023; Bernardini *et al.*, 2022; Salehi *et al.*, 2009; Salehi *et al.*, 2022; Gharouni-Kardani *et al.*, 2020; Esmailzadeh Hosseini *et al.*, 2018; Fernández *et al.*, 2018; Montano *et al.*, 2014; Lee *et al.*, 2012; Bertaccini *et al.*, 2005; Alma *et al.*, 2000; Gautam *et al.*, 2020). In Egypt, phytoplasma was found as *Candidatus* phytoplasma *asteris* infecting lilies (*Lilium* spp.) (Abdel-Salam *et al.*, 2022), gazania phyllody disease (Gad *et al.*, 2019), aster yellows phytoplasma affecting *Cycas revoluta* (Behiry, 2018) and rose phyllody disease (Mikhail *et al.*, 2012). In the Spring of 2021-2022, phytoplasma symptoms were noticed on African daisy (*Dimorphotheca pluvialis* L. Moench) plants grown in Cairo governorate, showing the phyllody and virescence of flowers as typical to symptoms observed on African daisy phyllody disease, these symptoms are observed for the first time in Egypt as we could not find any studies about phytoplasma

associated with phyllody disease in African daisy plants in Egypt.

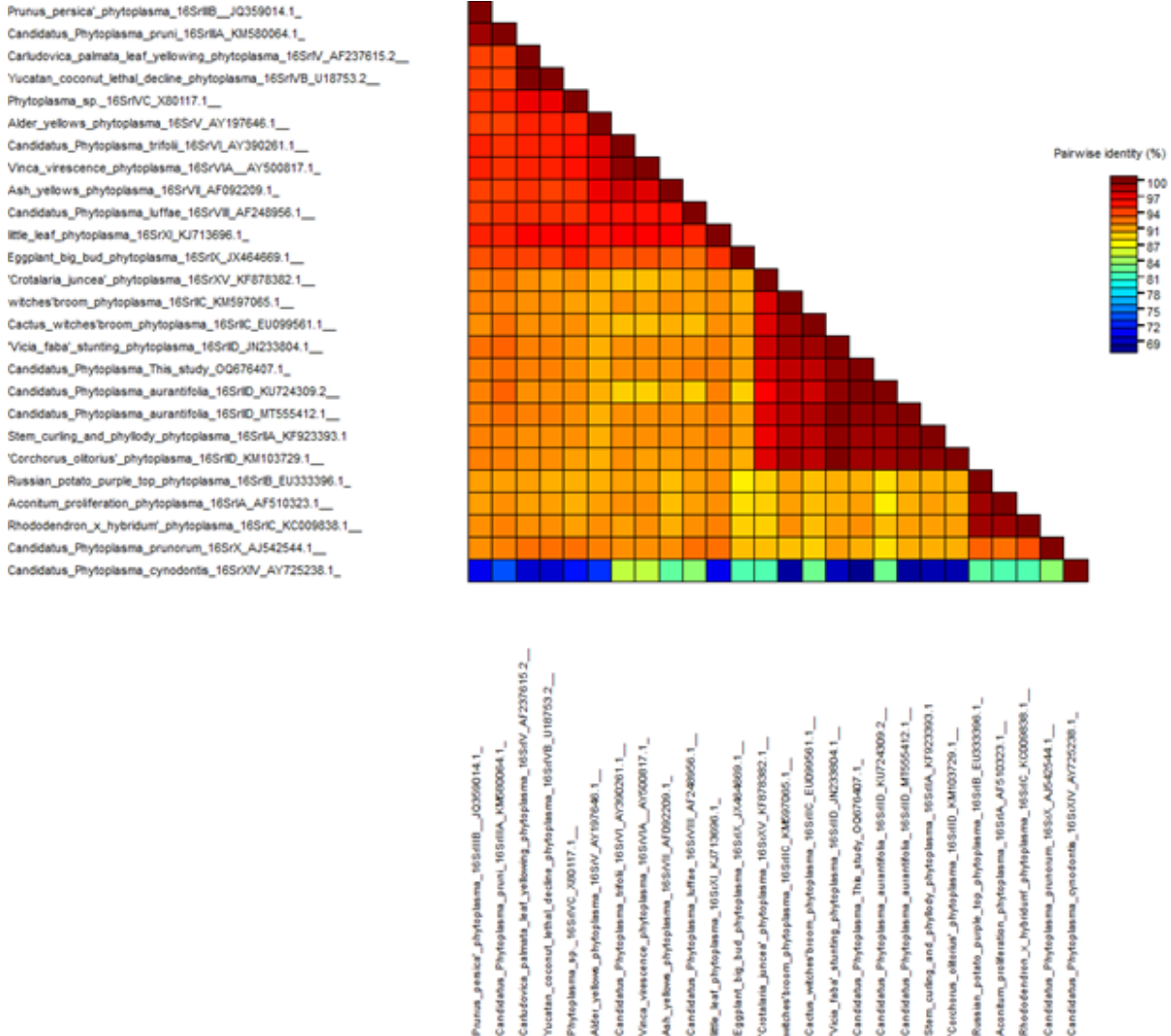


Figure 10. The percentage of nucleotide identities of the 16S ribosomal RNA (16S rRNA) gene of Dimo-Cairo isolate was calculated using Sequence Demarcation tool (SDT v1.3). Only one African daisy plant with phyllody disease was sequenced, due to our laboratory limited funding.

Phytoplasma-induced symptoms were successfully transmitted from naturally infected African daisy plants to healthy periwinkle ones in the greenhouse of the Virus and Phytoplasma Research Department, Plant Pathology Research Institute, Agricultural Research Center (ARC), Giza, Egypt using dodder transmissions as described by El-Banna *et al.* (2015), with 90% as the efficiency percentage of transmission, that was within the range reported by Ranebennur *et al.* (2022), who noticed the dodder transmission of sesame phyllody disease was reached to be 93.33% (sesame to sesame) and 92.85% (sesame to periwinkle). The exhibited

phyllody symptoms were very similar to the previous studies on the transmission phytoplasma using the parasitic dodder plant, such as gazania phyllody disease in gazania plants (Gad *et al.*, 2019), *Calendula officinalis* phyllody disease (Esmailzadeh Hosseini *et al.*, 2018), rose phyllody disease (Mikhail *et al.*, 2012), sesame phyllody disease (Ranebennur *et al.*, 2022) and safflower phyllody phytoplasma (Salehi *et al.*, 2009). Phytoplasma-infected African daisy plants, exhibited many ultrastructural changes in the vascular bundles with clearly thickness of the cell walls and many necrotic areas between phloem cells in the petioles midribs using

light microscopy as mentioned by El-Banna *et al.* (2015). Sometimes a lot of xylems exhibited in some vascular bundles. These induced anatomical changes were very close to corresponding with El-Banna and El-Deeb (2007), Randall *et al.* (2011) and Gad *et al.* (2019). As many investigators, such similar necrotic areas with/without producing new xylem cells were observed by Uehara *et al.* (1999), who were working on detection of Lettuce yellows phytoplasma in the garland chrysanthemum (cv. Kiwamechuyou) plants with ultrathin sections using light microscopy and was attributed to the infection of the plants by phytoplasma. Ultrathin sections of the petioles midribs tissues were re-evaluated visualized using the transmission electron microscope (TEM) which revealed numerous phytoplasma units with pleomorphic bodies in groups linked to the cell membrane as mentioned by El-Banna *et al.* (2015). The average of the phytoplasma units was high in the phloem parenchyma whereas the budding stage of phytoplasma was low also described by El-Banna *et al.* (2007), El-Banna *et al.* (2015) and Bernardini *et al.* (2022). In contrast to, Kamińska *et al.* (2001) noticed that there was no correlation between the number of the rose phyllody phytoplasma bodies and the severity of symptoms.

Phytoplasma infection caused various disorganization of the phloem components, such as cell wall thickening with a lot of growing extensions, necrotic areas between the phloem cells and vacuoles creating in the phloem parenchyma, all the above were recorded by El-Banna *et al.* (2015) who were working with citrus witches broom disease, and they attributed the thickness of the cell walls to the phytoplasma infection (Kamińska *et al.*, 2001), the presence of vacuoles to autophagic activity (Singh *et al.*, 2011), the accumulation of sugars and starch, which disturbs sieve tube functionality and disrupts phloem transport (Maust *et al.*, 2003).

The affected chloroplasts with destroyed grana arrangements, was confirmed with Fránová *et al.* (2003), who noticed swollen and degenerated chloroplasts with less amount of granal thylakoids in infected phloem tissues of strawflower (*Helichrysum bracteatum*) yellows phytoplasma, due to the down regulation of genes that are involved in the photosynthesis process (Xue *et al.*, 2018), causing photosynthetic process inhibition and thus abnormal carbohydrate accumulation in the infected plants.

The full length of 16S rRNA gene DNA fragments of

Dimorphotheca pluvialis phyllody phytoplasma (Dimo-Cairo) from all three Egyptian isolates were 1250 bp in size. Such a value is within the range recorded by other authors for phytoplasma in the ornamental plants, such as rose (Mikhail *et al.*, 2012), pot marigold (*Calendula officinalis*) (Esmailzadeh Hosseini *et al.*, 2018; Gharouni-Kardani *et al.*, 2020), gazania (Gad *et al.*, 2019), *Coreopsis grandiflora* (Gharouni-Kardani *et al.*, 2020), *Dodonaea viscosa* (Mokbel, 2020), lily (*Lilium* spp.) (Abdel-Salam *et al.*, 2022) and narrowleaf firethorn (*Pyracantha angustifolia*) plants (Kilic *et al.*, 2022).

Dimo-Cairo was directly sequenced and deposited in GenBank under accession number (OQ676407.1). Phylogenetic tree indicated that it is connected more closely with 16Sr-II group, because it shared 99.2% sequence homology with *Candidatus* Phytoplasma *aurantifolia* (Access no. KU724309.2) from Iraq according to Wei and Zhao (2022), who recognized phytoplasma as a novel '*Ca. Phytoplasma*' species if it is sharing <98.65% 16S rRNA gene sequence identity of the reference strains for phytoplasmas described either at the '*Candidatus*' level or at the 16S rRNA group/subgroup level (Duduk and Bertaccini, 2011).

AUTHOR CONTRIBUTIONS

All the authors have contributed equally to the research and compiling the data as well as editing the manuscript.

CONFLICTS OF INTEREST

The authors declare that there are no conflicts of interest.

REFERENCES

- Abdel-Salam, A. M., N. T. Shanan, D. Z. Soliman and M. A. Ahmed. 2022. First report of *Candidatus Phytoplasma Asteris* infecting lily in Egypt. Egyptian Academic Journal of Biological Sciences. C, Physiology and Molecular Biology, 14: 381-88.
- Alma, A., C. Marzachi, M. d'Aquilio and D. Bosco. 2000. Cyclamen (*Cyclamen persicum* L.): A dead-end host species for 16Sr-IB and-IC subgroup phytoplasmas. Annals of Applied Biology, 136: 173-78.
- Babaei, G., S. A. Esmailzadeh-Hosseini, S. Davoodi and A. Bertaccini. 2021. Occurrence and molecular characterization of a 16SrI-R subgroup phytoplasma associated with *Aquilegia vulgaris* phyllody disease. Journal of Plant Protection

- Research, 61: 222-28.
- Behiry, I. S. 2018. Characterization of aster yellows phytoplasma affecting *Cycas revoluta* in Egypt. *Journal of Plant Protection and Pathology*, 9: 591-94.
- Bernardini, C., S. Santi, G. Mian, A. Levy, S. Buoso, J. H. Suh, Y. Wang, C. Vincent, A. J. van Bel and R. Musetti. 2022. Increased susceptibility to chrysanthemum yellows phytoplasma infection in Atcals7ko plants is accompanied by enhanced expression of carbohydrate transporters. *Planta*, 256: 43.
- Bertaccini, A., J. Fránová, S. Botti and D. Tabanelli. 2005. Molecular characterization of phytoplasmas in lilies with fasciation in the Czech Republic. *FEMS Microbiology Letters*, 249: 79-85.
- Dehestani, A. and S. K. Tabar. 2007. A rapid efficient method for DNA isolation from plants with high levels of secondary metabolites. *Asian Journal of Plant Sciences*, 6: 977-81.
- Deng, S. and C. Hiruki. 1991. Amplification of 16S rRNA genes from culturable and nonculturable mollicutes. *Journal of Microbiological Methods*, 14: 53-61.
- Duduk, B. and A. Bertaccini. 2011. Phytoplasma classification: Taxonomy based on 16S ribosomal gene, is it enough? *Phytopathogenic Mollicutes*, 1: 3-13.
- El-Banna, O.-H. M. and S. H. El-Deeb. 2007. Phytoplasma associated with mango malformation disease in Egypt. *Journal of Phytopathology*, 35: 141-53.
- El-Banna, O.-H. M., A. A. Kheder, M. A. H. Ali, A. M. Sayed and G. M. Haseeb. 2020. Biological and molecular characterization of different egyptian isolates of *Spiroplasma citri*. *Plant Arch*, 20: 6457-69.
- El-Banna, O.-H. M., M. Mikhail, A. G. Farag and A. M. S. Mohammed. 2007. Detection of phytoplasma in tomato and pepper plants by electron microscopy and molecular biology based methods. *Egyptian Journal of Virology*, 4: 93-111.
- El-Banna, O.-H. M., N. I. Toima, S. A. Youssef and A. A. Shalaby. 2015. Molecular and electron microscope evidence for an association of phytoplasma with citrus witches broom disease. *International Journal of Scientific and Engineering Research*, 6: 127-33.
- Esmailzadeh Hosseini, S. A., M. Salehi, G. Babaie and A. Bertaccini. 2018. Characterization of a 16SrII subgroup D phytoplasma strain associated with *Calendula officinalis* phyllody in Iran. *3 Biotech*, 8: 1-6.
- Fernández, F., A. Uset, G. Baumgratz and L. Conci. 2018. Detection and identification of a 16SrIII-J phytoplasma affecting cassava (*Manihot esculenta* Crantz) in Argentina. *Australasian Plant Disease Notes*, 13: 1-5.
- Fránová, J., J. Příbylová, M. Šimková, M. Navrátil and P. Válová. 2003. Electron microscopy and molecular characterization of phytoplasmas associated with strawflower yellows in the Czech Republic. *European Journal of Plant Pathology*, 109: 883-87.
- Gad, S. M., A. A. Kheder and M. A. Awad. 2019. Detection and molecular identification of phytoplasma associated with *Gazania* in Egypt. *Journal of Virological Sciences*, 6: 12-23.
- Gautam, K. K., S. Kumar and S. K. Raj. 2020. Diseases affecting gerbera cultivation and their control measures. *The Journal of the Greens and Gardens*, 3: 1-16.
- Gharouni-Kardani, S., M. Ashnayi and A. Bertaccini. 2020. Detection of 16SrVI and 16SrIX phytoplasma groups in pot marigold and tickseed plants in northeastern Iran. *Folia Microbiologica*, 65: 697-703.
- Gundersen, D. and I.-M. Lee. 1996. Ultrasensitive detection of phytoplasmas by nested-PCR assays using two universal primer pairs. *Phytopathologia Mediterranea*, 35: 144-51.
- Hunter, E. E., P. Maloney and M. Bendayan. 1993. *Practical electron microscopy: A beginner's illustrated guide*. Cambridge University Press.
- Kamińska, M., H. Śliwa and A. Rudzińska-Langwald. 2001. The association of phytoplasma with stunting, leaf necrosis and witches' broom symptoms in magnolia plants. *Journal of Phytopathology*, 149: 719-24.
- Kilic, N., H. Ayvaci, M. E. Güldür and M. Dikilitas. 2022. First report of 'Candidatus *Phytoplasma australasia*'-related strain'(16SrII-D) in *Pyracantha angustifolia* (narrowleaf firethorn). *Australasian Plant Disease Notes*, 18: 1-9.
- Lee, G.-W., T.-W. Han, S. K. Lee and S.-S. Han. 2022. *Candidatus phytoplasma malaysianum* (16SrXXXII) associated with *Elaeocarpus sylvestris*

- decline in South Korea. *Forest Science and Technology*, 18: 7-13.
- Lee, I.-M., R. E. Davis and D. E. Gundersen-Rindal. 2000. Phytoplasma: Phytopathogenic mollicutes. *Annual Reviews in Microbiology*, 54: 221-55.
- Lee, S.-H., C.-e. Kim and B.-J. Cha. 2012. Migration and distribution of graft-inoculated jujube witches'-broom phytoplasma within a *Cantharanthus roseus* plant. *The Plant Pathology Journal*, 28: 191-96.
- Maust, B., F. Espadas, C. Talavera, M. Aguilar, J. M. Santamaría and C. Oropeza. 2003. Changes in carbohydrate metabolism in coconut palms infected with the lethal yellowing phytoplasma. *Phytopathology*, 93: 976-81.
- Mikhail, M., O.-H. El-Banna, E. Khalifa and A. Mohammed. 2012. Detection and control of rose phytoplasma phyllody disease. *Egyptian Journal of Phytopathology*, 40: 87-100.
- Mitra, S., P. Debnath, N. S. Radhika, E. P. Koshy and G. P. Rao. 2020. Aster yellows phytoplasmas association with a little leaf disease of papaya in Kerala, India. *Phytopathogenic Mollicutes*, 10: 188-93.
- Mokbel, S. A. 2020. Identification, molecular characterization of a phytoplasma affecting *dodonaea viscosa* plants and determination of some biochemical constituents in leaves. *Current Science International*, 9: 517-28.
- Montano, H. G., A. Bertaccini, J. P. Pimentel, S. Paltrinieri and N. Contaldo. 2014. *Erigeron (Conyza) bonariensis*, a host of '*Candidatus Phytoplasma fraxini*'-related strain in Brazil. *Phytopathogenic Mollicutes*, 4: 72-76.
- Muhire, B. M., A. Varsani and D. P. Martin. 2014. SDT: A virus classification tool based on pairwise sequence alignment and identity calculation. *Plos One*, 9: e108277.
- Randall, J. J., P. W. Bosland and S. F. Hanson. 2011. Brote grande, a new phytoplasma associated disease of chile peppers in the desert southwest. *Plant Health Progress*, 12: 18-26.
- Ranebennur, H., K. Rawat, A. Rao, P. Kumari, V. C. Chalam, N. Meshram and G. Rao. 2022. Transmission efficiency of a '*Candidatus Phytoplasma australasia*' (16SrII-D) related strain associated with sesame phyllody by dodder, grafting and leafhoppers. *European Journal of Plant Pathology*, 164: 193-208.
- Ravi, M., G. P. Rao, N. M. Meshram and R. Sundararaj. 2022. Genetic diversity of phytoplasmas associated with several Bamboo Species in India. *Forest Pathology*, 52: e12741.
- Salehi, E., M. Salehi, M. M. Faghihi and A. Bertaccini. 2022. Molecular characterization and transmission of a '*Candidatus Phytoplasma asteris*' strain associated with pot marigold phyllody in Iran. *Journal of Plant Pathology*, 104: 1457-64.
- Salehi, M., K. Izadpanah, M. Siampour, R. Firouz and E. Salehi. 2009. Molecular characterization and transmission of safflower phyllody phytoplasma in Iran. *Journal of Plant Pathology*, 91: 453-58.
- Salehi, M., N. Nejat, A. R. Tavakkoli and K. A. Izadpanah. 2005. Reaction of citrus cultivars to '*Candidatus phytoplasma aurantifolia*' in Iran. *Iranian Journal of Plant Pathology*, 41: 363-76.
- Shreenath, Y., A. Bahadur, H. Ranebennur and G. P. Rao. 2021. Characterization of '*Candidatus Phytoplasma asteris*'-related strain association with leaf yellowing of *Wrightia antidysenterica* (Arctic Snow) in Tripura, India. *Australasian Plant Disease Notes*, 16: 13-21.
- Sinclair, W. A., H. M. Griffiths and R. E. Davis. 1996. Ash yellows and lilac witches'-broom: phytoplasmal diseases of concern in forestry and horticulture. *Plant Disease*, 80: 468-75.
- Singh, M., Y. Chaturvedi, A. K. Tewari, G. P. Rao, S. K. Snehi, S. K. Raj and M. S. Khan. 2011. Diversity among phytoplasmas infecting ornamental plants grown in India. *Bulletin of Insectology*, 64: 69-70.
- Tamura, K., G. Stecher and S. Kumar. 2021. MEGA11: Molecular evolutionary genetics analysis version 11. *Molecular Biology and Evolution*, 38: 3022-27.
- Uehara, T., M. Tanaka, T. Shiomi, S. Namba, T. Tsuchizaki and I. Matsuda. 1999. Histopathological studies on two symptom types of phytoplasma associated with lettuce yellows. *Japanese Journal of Phytopathology*, 65: 465-69.
- Viczián, O., J. Fodor, J. Ágoston and E. Mergenthaler. 2023. First report of '*Candidatus Phytoplasma asteris*' associated with cyclamen little leaf in Hungary. *Plant Disease*, 107: 2515.
- Wei, W. and Y. Zhao. 2022. Phytoplasma taxonomy: Nomenclature, classification, and identification.

Biology, 11: 1119.

Xue, C., Z. Liu, L. Dai, J. Bu, M. Liu, Z. Zhao, Z. Jiang, W. Gao
and J. Zhao. 2018. Changing host photosynthetic,

carbohydrate, and energy metabolisms play
important roles in phytoplasma infection.
Phytopathology, 108: 1067-77.

Publisher's note: ESscience Press remains neutral with regard to jurisdictional claims in published maps and institutional affiliations.



Open Access This article is licensed under a Creative Commons Attribution 4.0 International License, which permits use, sharing, adaptation, distribution and reproduction in any medium or format, as long as you give appropriate credit to the original author(s) and the source, provide a link to the Creative Commons license and indicate if changes were made. The images or other third-party material in this article are included in the article's Creative Commons license, unless indicated otherwise in a credit line to the material. If material is not included in the article's Creative Commons license and your intended use is not permitted by statutory regulation or exceeds the permitted use, you will need to obtain permission directly from the copyright holder. To view a copy of this license, visit <http://creativecommons.org/licenses/by/4.0/>.